

Ordering of the Heisenberg Spin Glass in Two Dimensions

Hikaru Kawamura and Hitoshi Yonehara¹

¹*Department of Earth and Space Science, Faculty of Science, Osaka University, Toyonaka 560-0043, Japan*

(Dated: November 4, 2018)

The spin and the chirality orderings of the Heisenberg spin glass in two dimensions with the nearest-neighbor Gaussian coupling are investigated by equilibrium Monte Carlo simulations. Particular attention is paid to the behavior of the spin and the chirality correlation lengths. In order to observe the true asymptotic behavior, fairly large system size $L \gtrsim 20$ (L the linear dimension of the system) appears to be necessary. It is found that both the spin and the chirality order only at zero temperature. At high temperatures, the chiral correlation length stays shorter than spin correlation length, whereas at lower temperatures below the crossover temperature T_\times , the chiral correlation length exceeds the spin correlation length. The spin and the chirality correlation-length exponents are estimated above T_\times to be $\nu_{\text{SG}} = 0.9 \pm 0.2$ and $\nu_{\text{CG}} = 2.1 \pm 0.3$, respectively. These values are close to the previous estimates on the basis of the domain-wall-energy calculation. Discussion is given about the asymptotic critical behavior realized below T_\times .

INTRODUCTION

Spin glasses (SGs) are the type of random magnets possessing both the ferromagnetic and the antiferromagnetic couplings, and are characterized both by frustration and randomness. Experimentally, it is now well established that typical SG magnets exhibit an equilibrium phase transition at a finite temperature and that there exists a thermodynamic SG phase. The true nature of the SG transition and of the SG ordered phase, however, has not fully been understood yet in spite of extensive studies for years.

In numerical studies of SGs, much effort has been devoted to clarify the properties of the so-called Edwards-Anderson (EA) model [1]. Most of these numerical works on the EA model have concentrated on the *Ising* EA model. By contrast, many of real SG magnets are Heisenberg-like rather than Ising-like in the sense that the magnetic anisotropy is considerably weaker than the isotropic exchange interaction [1, 2]. Presumably, theoretical bias toward the Ising model is partly due to the simplicity of the Ising model, but partly also reflects the historical situation that the earlier theoretical studies on the Heisenberg EA model strongly suggested in common that the Heisenberg EA model did not exhibit any finite-temperature transition [2, 3, 4, 5, 6], apparently making it difficult in explaining the experimental SG transition within the isotropic Heisenberg model.

Meanwhile, a novel possibility was suggested by one of the present authors (H.K.) that the 3D Heisenberg SG might exhibit an equilibrium phase transition at a finite temperature, not in the spin sector as usually envisaged, but in the *chirality* sector, *i.e.*, might exhibit a *chiral-glass* (CG) transition [7]. Chirality is a multi-spin variable representing the sense or the handedness of local noncoplanar spin structures induced by spin frustration. In the CG ordered state, chiralities are ordered in a spatially random manner while Heisenberg spins remain paramagnetic. Refs. [7, 8, 9, 10, 11, 12] claimed

that the standard SG order associated with the freezing of the Heisenberg spin occurred at a temperature lower than the CG transition temperature at $T = T_{\text{SG}} < T_{\text{CG}}$, quite possibly $T_{\text{SG}} = 0$. It means that the spin and the chirality are decoupled on long length scales (spin-chirality decoupling). In fact, based on such a spin-chirality decoupling picture, a chirality scenario of the SG transition has been advanced, which explains the experimentally observed SG transition as essentially chirality driven [7, 9]. Note that the numerical observation of a finite-temperature CG transition in the 3D Heisenberg SG [7, 8, 9, 10, 11, 12] is not inconsistent with the earlier observations of the absence of the conventional SG order at any finite temperature.

Recently, however, in a series of numerical studies on the 3D Heisenberg EA model, Tohoku group criticized the earlier numerical works, claiming that in the 3D Heisenberg SG the spin ordered at a finite temperature and that the SG transition temperature might coincide with the CG transition temperature, *i.e.*, $T_{\text{SG}} = T_{\text{CG}} > 0$ [13, 14]. By calculating the spin and the chirality correlation lengths, Lee and Young also suggested $T_{\text{SG}} = T_{\text{CG}} > 0$ [15]. By contrast, Hukushima and Kawamura maintained that in 3D the spin and the chirality were decoupled on sufficiently long length scales, and that $T_{\text{SG}} < T_{\text{CG}}$ [16], supporting the earlier numerical results. The situation in 3D thus remains controversial.

Under such circumstances, in order to shed further light on the nature of the ordering in 3D, it might be useful to study the problem for the general space dimensionality D . The spin and the chirality orderings of the Heisenberg SG in dimensions higher than three, *i.e.*, 4D, 5D and $D = \infty$ (an infinite-ranged mean-field SG model), were recently studied in Ref.[17]. In the present paper, we wish to study the spin and the chirality orderings of the low-dimensional system, *i.e.*, the Heisenberg SG in 2D.

There were only a few theoretical and numerical works performed for the 2D Heisenberg EA model. On ana-

lytical side, there exists a proof that the standard SG long-range order (LRO) does not arise at any finite temperature [18]. The proof, however, does not tell whether the CG LRO could exist or not in 2D. On numerical side, the domain-wall-energy calculation suggested that both the spin and the chirality ordered only at $T = 0$, but with mutually different correlation-length exponents, $\nu_{\text{CG}} \sim 2.1 > \nu_{\text{SG}} \sim 1.0 - 1.2$ [7]. If this is really the case, the spin and the chirality are decoupled on long length scale at the $T = 0$ transition. We note that a similar phenomenon has also been reported for the 2D XY SG [19, 20, 21, 22]. Meanwhile, to the authors' knowledge, no Monte Carlo (MC) simulation for the 2D Heisenberg SG has been reported so far.

In the present paper, we wish to fill this gap. We study both the SG and the CG orderings of the 2D Heisenberg EA model by means of a large-scale equilibrium MC simulation. The present paper is organized as follows. In §2, we introduce our model and explain some of the details of the MC calculation. Various physical quantities calculated in our MC simulations, *e.g.*, the SG and the CG susceptibilities, the spin and the chiral Binder ratios, the SG and the CG correlation functions and the associated correlation lengths are introduced in §3. The results of our MC simulations are presented and analyzed in §4. Section 5 is devoted to brief summary of the results.

THE MODEL AND THE METHOD

The model we consider is the isotropic classical Heisenberg model on a 2D square lattice with the nearest-neighbor Gaussian coupling. The Hamiltonian is given by

$$\mathcal{H} = - \sum_{\langle ij \rangle} J_{ij} \vec{S}_i \cdot \vec{S}_j \quad , \quad (1)$$

where $\vec{S}_i = (S_i^x, S_i^y, S_i^z)$ is a three-component unit vector, and the $\langle ij \rangle$ sum is taken over nearest-neighbor pairs on the lattice. The nearest-neighbor coupling J_{ij} is assumed to obey the Gaussian distribution with zero mean and variance J^2 . We perform equilibrium MC simulations on the model. The lattices studied are square lattices with $N = L^2$ sites with $L = 10, 16, 20, 30$ and 40 with periodic boundary conditions in all directions. Sample average is taken over 384 ($L = 10, 16, 20$) and 320 ($L = 30, 40$) independent bond realizations. Error bars of physical quantities are estimated by the sample-to-sample statistical fluctuation over the bond realizations.

In order to facilitate efficient thermalization, we combine the standard heat-bath method with the temperature-exchange technique [23]. Care is taken to be sure that the system is fully equilibrated. Equilibration is checked by the following procedures. First, we monitor

the system to travel back and forth many times along the temperature axis during the temperature-exchange process (typically more than 10 times) between the maximum and minimum temperature points. We check at the same time that the relaxation due to the standard heat-bath updating is reasonably fast at the highest temperature, whose relaxation time is of order 10^2 Monte Carlo steps per spin (MCS). This guarantees that different parts of the phase space are sampled in each "cycle" of the temperature-exchange run. Second, we check the stability of the results against at least three times longer runs for a subset of samples.

PHYSICAL QUANTITIES

In this section, we define various physical quantities calculated in our simulations below. By considering two independent systems ("replicas") described by the same Hamiltonian (1), one can define an overlap variable. The overlap of the Heisenberg spin is defined as a *tensor* variable $q_{\alpha\beta}$ between the α and β components ($\alpha, \beta = x, y, z$) of the Heisenberg spin,

$$q_{\alpha\beta} = \frac{1}{N} \sum_{i=1}^N S_{i\alpha}^{(1)} S_{i\beta}^{(2)} \quad , \quad (\alpha, \beta = x, y, z) \quad , \quad (2)$$

where $\vec{S}_i^{(1)}$ and $\vec{S}_i^{(2)}$ are the i -th Heisenberg spins of the replicas 1 and 2, respectively. In our simulations, we prepare the two replicas 1 and 2 by running two independent sequences of systems in parallel with different spin initial conditions and different sequences of random numbers. In terms of these tensor overlaps, the SG order parameter is defined by

$$q_s^{(2)} = [\langle q_s^2 \rangle] \quad , \quad q_s^2 = \sum_{\alpha, \beta = x, y, z} q_{\alpha\beta}^2 \quad , \quad (3)$$

and the SG susceptibility by

$$\chi_{\text{SG}}^{(2)} = N q_s^{(2)} \quad , \quad (4)$$

where $\langle \dots \rangle$ represents the thermal average and $[\dots]$ the average over the bond disorder. The associated spin Binder ratio is defined by

$$g_{\text{SG}} = \frac{1}{2} \left(11 - 9 \frac{[\langle q_s^4 \rangle]}{[\langle q_s^2 \rangle]^2} \right) \quad . \quad (5)$$

Note that g_{SG} is normalized so that, in the thermodynamic limit, it vanishes in the high-temperature phase and gives unity in the nondegenerate ordered state.

The local chirality at the i -th site and in the μ -th direction $\chi_{i\mu}$ may be defined for three neighboring Heisenberg spins by the scalar,

$$\chi_{i\mu} = \vec{S}_{i+\hat{e}_\mu} \cdot (\vec{S}_i \times \vec{S}_{i-\hat{e}_\mu}) \quad , \quad (6)$$

where \hat{e}_μ ($\mu = x, y$) denotes a unit vector along the μ -th axis. There are in total $2N$ local chiral variables. We define the mean local amplitude of the chirality, $\bar{\chi}$, by

$$\bar{\chi} = \sqrt{\frac{1}{2N} \sum_{i=1}^N \sum_{\mu=x,y} [\langle \chi_{i\mu}^2 \rangle]} . \quad (7)$$

Note that the magnitude of $\bar{\chi}$ tells us the extent of the noncoplanarity of the local spin structures. In particular, $\bar{\chi}$ vanishes for any coplanar spin configuration.

As in the case of the Heisenberg spin, one can define an overlap of the chiral variable by considering the two replicas by

$$q_\chi = \frac{1}{2N} \sum_{i=1}^N \sum_{\mu=x,y} \chi_{i\mu}^{(1)} \chi_{i\mu}^{(2)} , \quad (8)$$

where $\chi_{i\mu}^{(1)}$ and $\chi_{i\mu}^{(2)}$ represent the chiral variables of the replicas 1 and 2, respectively. In terms of this chiral overlap q_χ , the CG order parameter is defined by

$$q_\chi^{(2)} = [\langle q_\chi^2 \rangle] , \quad (9)$$

and the associated CG susceptibility by

$$\chi_{\text{CG}} = 2N[\langle q_\chi^2 \rangle] . \quad (10)$$

Unlike the spin variable, the local magnitude of the chirality is not normalized to unity, and is also temperature dependent somewhat. In order to take account of this effect, and also to get an appropriate normalization, we also consider the reduced CG susceptibility $\tilde{\chi}_{\text{CG}}$ by dividing χ_{CG} by appropriate powers of $\bar{\chi}$,

$$\tilde{\chi}_{\text{CG}} = \frac{\chi_{\text{CG}}}{\bar{\chi}^4} . \quad (11)$$

The Binder ratio of the chirality is defined by

$$g_{\text{CG}} = \frac{1}{2} \left(3 - \frac{[\langle q_\chi^4 \rangle]}{[\langle q_\chi^2 \rangle]^2} \right) . \quad (12)$$

The two-point SG correlation function is defined by

$$\begin{aligned} C_{\text{SG}}(\vec{r}) &= \frac{1}{N} \sum_i [\langle \vec{S}_i \cdot \vec{S}_{i+\vec{r}} \rangle^2], \\ &= \frac{1}{N} \sum_i \sum_{\alpha\beta} [\langle S_{i,\alpha}^{(1)} S_{i,\beta}^{(2)} S_{i+\vec{r},\alpha}^{(1)} S_{i+\vec{r},\beta}^{(2)} \rangle], \end{aligned} \quad (13)$$

where $\vec{r} = (x, y)$ denotes the two-dimensional positional vector between the two Heisenberg spins. The associated spin correlation length ξ_{SG} is defined, with $\hat{C}(\vec{k}) = \hat{C}(k_x, k_y)$ being the Fourier transform of $C(\vec{r})$, by

$$\xi_{\text{SG}} = \frac{1}{2 \sin(\frac{\pi}{L})} \sqrt{\frac{\hat{C}_0}{\hat{C}_m} - 1}, \quad (14)$$

$$\hat{C}_0 = \hat{C}(0, 0), \quad \hat{C}_m = \frac{1}{2} [\hat{C}(k_{\min}, 0) + \hat{C}(0, k_{\min})], \quad (15)$$

where $k_{\min} = \frac{2\pi}{L}$ is the minimum nonzero wavevector under the periodic boundary conditions.

Concerning the chirality correlation, we introduce the two-point CG correlation function $C_{\text{CG}}^{\mu\nu}(\vec{r})$ between the two local chiral variables in the μ -th and in the ν -th directions, which are apart by the positional vector \vec{r} , by

$$\begin{aligned} C_{\text{CG}}^{\mu\nu}(\vec{r}) &= \frac{1}{N} \sum_i [\langle \chi_{i,\mu} \chi_{i+\vec{r},\nu} \rangle^2], \\ &= \frac{1}{N} \sum_i [\langle \chi_{i,\mu}^{(1)} \chi_{i,\mu}^{(2)} \chi_{i+\vec{r},\nu}^{(1)} \chi_{i+\vec{r},\nu}^{(2)} \rangle]. \end{aligned} \quad (16)$$

We then define the following three types of chiral correlation lengths, ξ_{CG}^\perp , $\xi_{\text{CG}}^\parallel$ and ξ_{CG}^+ , depending on the relative directions of the local chiral variables with respect to the positional vector \vec{r} ,

$$\xi_{\text{CG}}^\perp = \frac{1}{2 \sin(\frac{\pi}{L})} \sqrt{\frac{\hat{C}_{\chi_0}^\perp}{\hat{C}_{\chi_m}^\perp} - 1}, \quad (17)$$

$$\xi_{\text{CG}}^\parallel = \frac{1}{2 \sin(\frac{\pi}{L})} \sqrt{\frac{\hat{C}_{\chi_0}^\parallel}{\hat{C}_{\chi_m}^\parallel} - 1}, \quad (18)$$

$$\xi_{\text{CG}}^+ = \frac{1}{2 \sin(\frac{\pi}{L})} \sqrt{\frac{\hat{C}_{\chi_0}^+}{\hat{C}_{\chi_m}^+} - 1}, \quad (19)$$

where the $k = 0$ Fourier components $C_{\chi,0}^\perp$, $C_{\chi,0}^\parallel$ and $C_{\chi,0}^+$, are given by

$$\hat{C}_{\chi_0}^\perp = \hat{C}_{\chi_0}^\parallel = \frac{1}{2} [\hat{C}^{xx}(0, 0) + \hat{C}^{yy}(0, 0)], \quad (20)$$

$$\hat{C}_{\chi_0}^+ = \frac{1}{2} [\hat{C}^{xy}(0, 0) + \hat{C}^{yx}(0, 0)], \quad (21)$$

while the $k = k_{\min}$ components $C_{\chi_m}^\perp$, $C_{\chi_m}^\parallel$ and $C_{\chi_m}^+$ are given by

$$\hat{C}_{\chi_m}^\perp = \frac{1}{2} [\hat{C}^{yy}(k_{\min}, 0) + \hat{C}^{xx}(0, k_{\min})], \quad (22)$$

$$\hat{C}_{\chi_m}^\parallel = \frac{1}{2} [\hat{C}^{xx}(k_{\min}, 0) + \hat{C}^{yy}(0, k_{\min})], \quad (23)$$

$$\begin{aligned} \hat{C}_{\chi_m}^+ &= \frac{1}{4} [\hat{C}^{xy}(k_{\min}, 0) + \hat{C}^{yx}(k_{\min}, 0) \\ &\quad + \hat{C}^{xy}(0, k_{\min}) + \hat{C}^{yx}(0, k_{\min})]. \end{aligned} \quad (24)$$

In these configurations, the directions of the two chiralities are, (i) both perpendicular to the positional vector for ξ_{CG}^\perp , (ii) both parallel with the positional vector for $\xi_{\text{CG}}^\parallel$, and (iii) one perpendicular to, and one parallel with the positional vector for ξ_{CG}^+ .

MONTÉ CARLO RESULTS

In this section, we present our MC results. In Fig.1, we show the temperature dependence of (a) the SG susceptibility χ_{SG} , and of (b) the reduced CG susceptibility $\tilde{\chi}_{CG}$ (b), on a log-log plot. Recall that the SG transition temperature of the present model is expected to be at $T = 0$. As can be seen from Fig.1(a), our data of χ_{SG} is consistent with a power-law divergence at zero temperature, $\chi_{SG} \approx T^{-\gamma_{SG}}$, with an exponent $\gamma_{SG} \simeq 1.5 - 1.8$. In Fig.1(a), a straight line with a slope equal to -1.8 is drawn, which is the best γ_{SG} value determined from the other physical quantities analyzed below. We note that the size dependence of χ_{SG} is normal in the sense that χ_{SG} gets larger as the system size L is increased, and that this tendency is enhanced at temperatures closer to $T_{SG} = 0$.

By contrast, the size dependence of the CG susceptibility is somewhat unusual: In the temperature range $T/J \gtrsim 0.025$, χ_{CG} gets smaller as L is increased, contrary to the tendency normally expected for a diverging quantity in the critical region. At lower temperatures $T/J \lesssim 0.025$, the size dependence of $\tilde{\chi}_{CG}$ is changed into the normal one, *i.e.*, it gets larger as L is increased. Although there is no proof that the CG transition temperature of the model is $T_{CG} = 0$, if one fits the data to a power-law divergence of the form, $\chi_{CG} \approx T^{-\gamma_{CG}}$, assuming $T_{CG} = 0$, one gets $\gamma_{CG} \simeq 4.0$: See Fig.1(b) The CG susceptibility exponent γ_{CG} is then more than twice the SG susceptibility exponent $\gamma_{SG} \simeq 1.8$.

For any $T = 0$ transition with a nondegenerate ground state, the critical-point-decay exponent η should be given by $\eta = 2 - d$ (d the space dimensionality), which leads to the scaling relation $\gamma = d\nu = 2\nu$ (for $d = 2$) between the susceptibility exponent γ and the associated correlation-length exponent ν . Hence, mutually different susceptibility exponents for the spin and for the chirality necessarily mean mutually different correlation-length exponents for the spin and for the chirality, *i.e.*, $\nu_{SG} \simeq 0.9$ and $\nu_{CG} \simeq 2.0$. This apparently indicates the spin-chirality decoupling. However, one should be careful that the present data of the SG and CG susceptibilities alone are not enough to completely exclude the possibility that the critical behavior crosses over to a different one at still lower temperatures, or even the possibility of the occurrence of a finite-temperature CG transition.

In order get further information, we show in Fig. 2 (a) the Binder ratio of the spin g_{SG} , and (b) of the chirality g_{CG} . As can be seen from Fig.2(a), the spin Binder ratio for smaller sizes $L \leq 20$ exhibits a crossing at a nonzero temperature, while the crossing temperatures tend to shift to lower temperatures with increasing L . For larger sizes $L \geq 20$, by contrast, g_{SG} does not exhibit a crossing at any temperature studied, always getting smaller with increasing L . Such a behavior is indeed con-

sistent with the expected $T = 0$ SG transition. Another point to be noticed is that g_{SG} for larger sizes exhibits a wavy structure at around $0.02 \lesssim T/J \lesssim 0.03$, suggesting the occurrence of some sort of changeover in the ordering behavior.

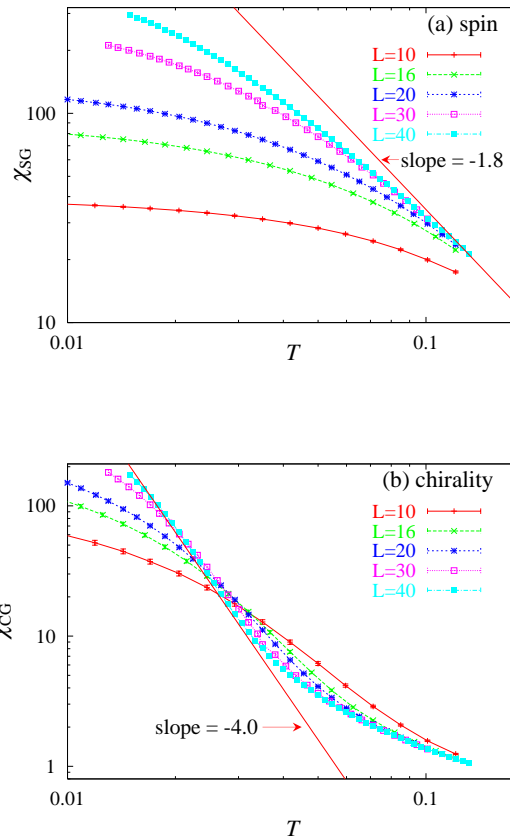


FIG. 1: Temperature dependence of (a) the spin-glass susceptibility, and (b) the reduced chiral-glass susceptibility (b), on a log-log plot.

Similarly to the spin Binder ratio, the chiral Binder ratio for smaller sizes $L \leq 20$ also exhibits a crossing at a nonzero temperature, where the crossing temperatures tend to shift to lower temperatures with increasing L . For larger sizes $L \geq 20$, by contrast, g_{CG} does not exhibit a crossing at any temperature studied, always getting smaller with increasing L . Such a behavior strongly suggests that the CG transition occurs only at $T = 0$. A closer look of the data reveals that g_{CG} exhibits a shallow negative dip at a size-dependent temperature $T_{dip}(L)$, which tends to become shallower with increasing L . Although such a negative dip is also observed in the 3D Heisenberg SG, it tends to become deeper in the 3D case in contrast to the present 2D case[10]. As argued in Ref.[10], if a negative dip persists in the $L \rightarrow \infty$ limit with $T_{dip}(L = \infty) > 0$, it means the occurrence of a finite-temperature CG transition at

$T = T_{CG} = T_{dip}(L = \infty)$. In the present 2D case, however, the observed $T_{dip}(L)$ decreases rapidly with increasing L , tending to $T = 0$ in the $L \rightarrow \infty$ limit. Indeed, a fit of our data of $T_{dip}(L)$ to the form, $T_{dip}(\infty) + \text{const.}/L$, yields an estimate $T_{dip}(\infty)/J = 0.00 \pm 0.01$. Thus, we conclude again that the CG transition of the present 2D model occurs only at $T = 0$, simultaneously with the SG transition.

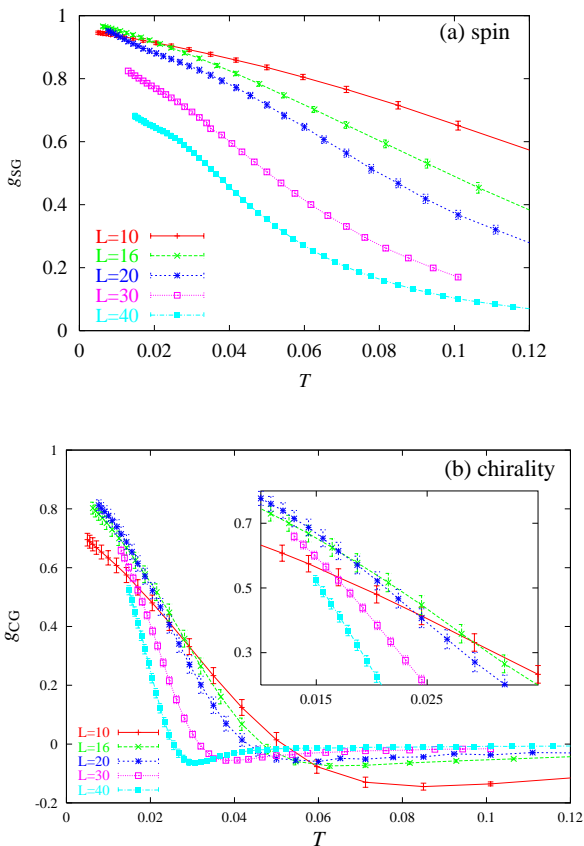


FIG. 2: Temperature dependence of (a) the spin Binder ratio, and (b) the chiral Binder ratio. The inset is a magnified view of the low-temperature region.

Next, we show our data of the correlation lengths. Fig.3 exhibits the temperature and size dependence of the SG correlation length ξ_{SG} . One sees from the figure that ξ_{SG} exhibits a diverging behavior toward the zero-temperature transition point. We note that the size dependence of ξ_{SG} is normal, always getting larger with increasing L .

Figs. 4(a)-(c) exhibit the temperature and size dependence of the three distinct types of the CG correlation lengths, ξ_{CG}^{\perp} , ξ_{CG}^{\parallel} and ξ_{CG}^{+} , defined above. As can be seen from the figures, these three chirality correlation lengths exhibit very much similar behaviors. They all show a diverging behavior toward the $T = 0$ transition point, accompanied by similar size dependence. While

they all show normal size dependence at lower temperatures $T/J \lesssim 0.03$, increasing with L , they all show unusual size dependence in the range $T/J \gtrsim 0.03$, decreasing with L .

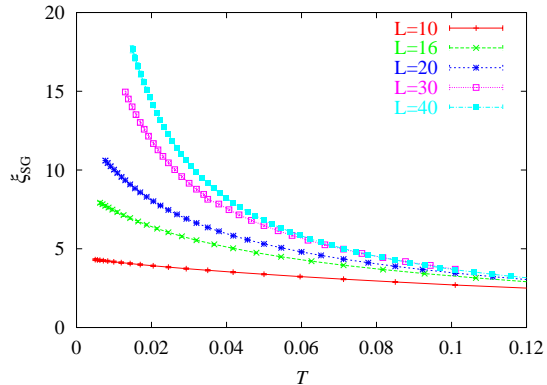


FIG. 3: Temperature dependence of the spin-glass correlation length.

In order to compare the SG and the CG correlation lengths more quantitatively, we plot in Fig.5 ξ_{SG} together with ξ_{CG}^{+} , which is the longest one among the three types of CG correlation lengths. At higher temperatures, the chiral correlation length is shorter than the SG correlation length. This simply reflects the fact that the short-range correlation of the spins is a prerequisite for the onset of any chiral order. As the temperature is decreased, ξ_{CG} grows much faster than ξ_{SG} , then catches up and eventually exceeds ξ_{SG} at a size-dependent temperature $T_{\times}(L)$. This behavior suggests that the chirality orders more strongly than the spin. As shown in Fig.5, the linear fit of the log-log plot of the data yields slopes $\nu_{SG} = 0.9 \pm 0.2$ for ξ_{SG} , and $\nu_{CG} = 2.2 \pm 0.3$ for ξ_{CG} , the latter being more than twice the former. These values are consistent with our estimates of the SG and CG susceptibility exponents given above, $\gamma_{SG} = 2\nu_{SG} \simeq 1.8$ and $\gamma_{CG} = 2\nu_{CG} \simeq 4.0$.

We note that the crossover temperatures $T_{\times}(L)$ where ξ_{CG} exceeds ξ_{SG} tend to decrease with increasing L . We get $T_{\times}/J \simeq 0.025, 0.019, 0.017, 0.012$ and 0.012 for $L = 10, 16, 20, 30$ and 40 , respectively (for $L = 30$ and 40 , we have extrapolated the data slightly to lower temperatures to estimate T_{\times}). In particular, if $T_{\times}(L)$ would tend to zero as $L \rightarrow \infty$, the spin correlation would dominate the chiral correlation at any nonzero temperature. This seems not to be the case here, however, since the estimated T_{\times} for our two largest sizes $L = 30$ and 40 turn out to be almost the same, $T_{\times}/J \simeq 0.012$. Hence, the indication is that, even in an infinite system, ξ_{CG} exceeds ξ_{SG} at low enough temperatures $T < T_{\times} \sim 0.01J$, where the chiral correlation dominates the spin correlation. The nontrivial question still to be addressed is the

asymptotic critical behaviors of ξ_{SG} and of ξ_{CG} realized below T_x . Although it is difficult to say something definite in this regime because of the lack of the data, we will discuss this point later.

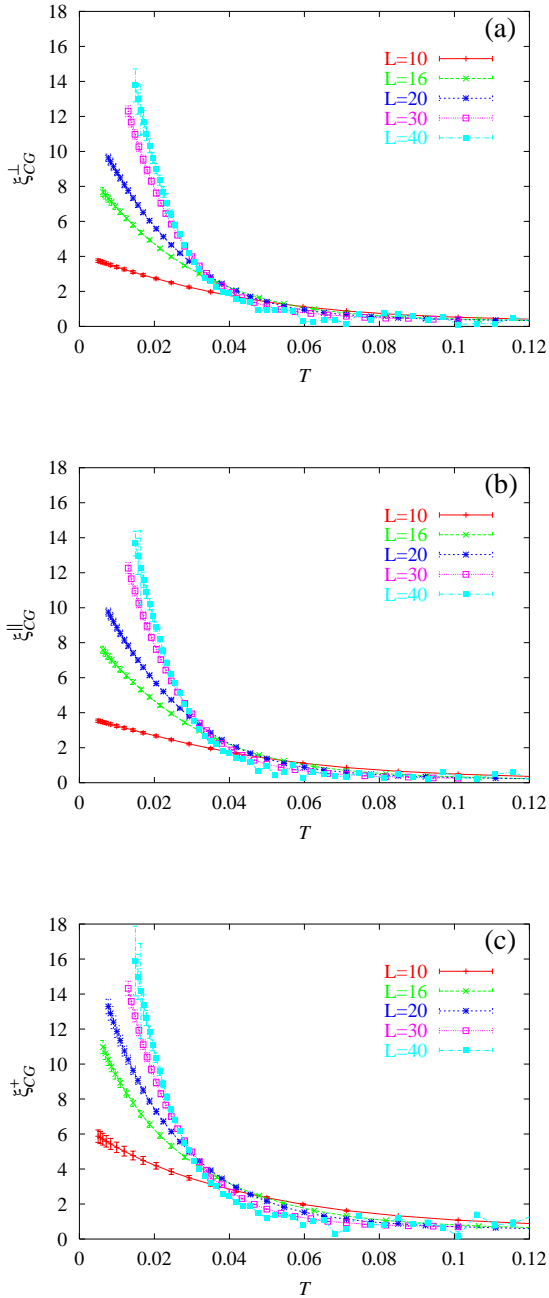


FIG. 4: Temperature dependence of the three types of the chiral-glass correlation lengths, Eqs.(17)-(19); (a) ξ_{CG}^\perp , (b) $\xi_{\text{CG}}^\parallel$, and (c) ξ_{CG}^+ .

In Fig.6(a), we show the temperature dependence of the dimensionless SG correlation length ξ_{SG}/L for several sizes. Somewhat unexpectedly, ξ_{SG}/L for smaller sizes

$L = 10, 16$ and 20 cross almost at a point $T/J \simeq 0.022$, giving an appearance of a finite-temperature SG transition. However, ξ_{SG}/L for larger sizes $L = 30$ and 40 changes its behavior: They gradually come down, without a crossing at $T/J = 0.022$. Hence, the behavior of ξ_{SG}/L for larger L is eventually consistent with the SG transition only at $T = 0$. However, we note that this behavior becomes evident only for larger sizes $L \gtrsim 20$, and one has to be careful in the interpretation of the ξ_{SG}/L data for smaller lattices. If one looked at the present ξ_{SG}/L data for smaller sizes only, say, for $L \leq 20$, one might easily misconclude that the SG transition of the model occurred at a nonzero temperature $T/J \simeq 0.022$.

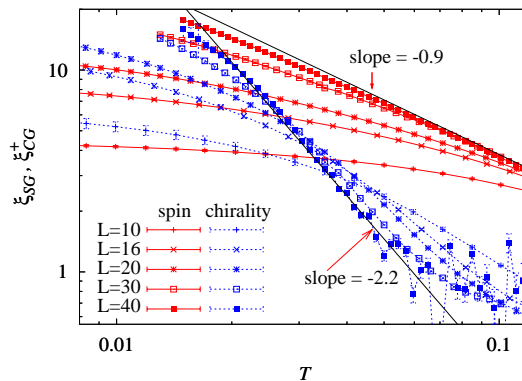


FIG. 5: Temperature dependence of the spin-glass correlation length ξ_{SG} as compared with the chiral-glass correlation length ξ_{CG}^+ on a log-log plot.

In Fig.6(b), we show the temperature dependence of the dimensionless CG correlation length ξ_{CG}/L for several sizes. Again, ξ_{SG}/L for smaller size exhibits a crossing at a nonzero temperature, while the crossing temperatures tend to shift down to lower temperatures in this case. The observed behavior is consistent with the occurrence of a $T = 0$ CG transition. We note that very much similar behaviors are found for the other types of the dimensionless CG correlation length, ξ_{CG}^\perp/L and $\xi_{\text{CG}}^\parallel/L$ (data not shown here).

Having established that both the SG and the CG transitions occur only at $T = 0$, we now analyze the critical properties associated with the $T = 0$ transition on the basis of a finite-size scaling. In the analysis below, we use the data only at lower temperatures $T/J \leq 0.024$ where the chirality enters into the critical regime exhibiting the normal size dependence, and for moderately large sizes $L \geq 20$. Since the exponent η associated with the $T = 0$ transition should be zero, we fix $T_{\text{SG}} = 0$, $T_{\text{CG}} = 0$, $\eta_{\text{SG}} = 0$ and $\eta_{\text{CG}} = 0$ below.

We begin with the chirality ordering. Fig.7(a) exhibits a finite-size scaling plot of the CG susceptibility, where the best value of ν_{CG} is estimated to be $\nu_{\text{CG}} = 2.0 \pm 0.3$.

The value of ν_{CG} is consistent with the one determined from the log-log plot of the CG susceptibility.

In Fig.7(b), we show a scaling plot of the chiral Binder ratio g_{CG} with $\nu_{CG} = 2.0$. The data collapse turns out to be reasonably good. In Fig.7(c), we show a scaling plot of the dimensionless chiral correlation length ξ_{CG}/L with $\nu_{CG} = 2.0$. The data collapse turns out to be marginally good. Hence, our data of the CG susceptibility, the chiral Binder ratio and the chiral correlation length seem all consistent with $\nu_{CG} = 2.0 \pm 0.3$. Taking account of the corresponding estimate based on Fig.5, we finally quote $\nu_{CG} = 2.1 \pm 0.3$ as our best estimate of ν_{CG} .

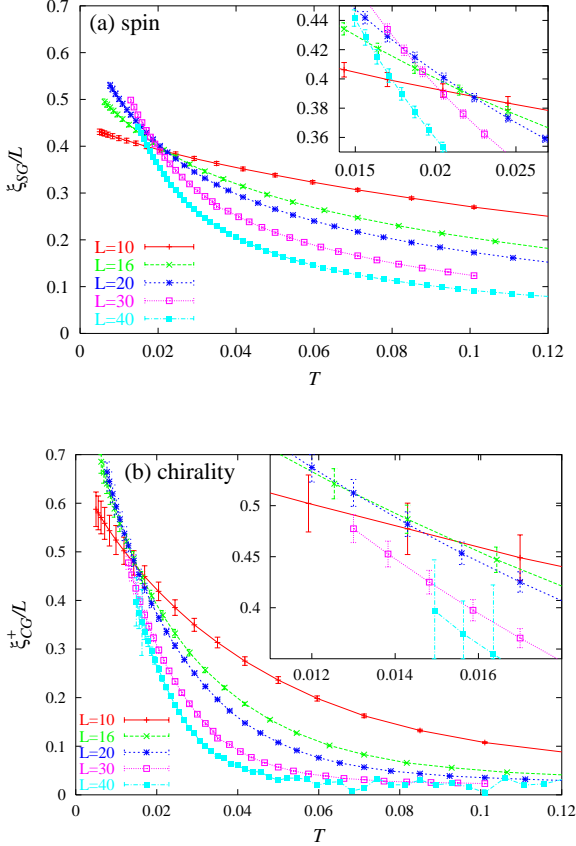


FIG. 6: Temperature and size dependence of (a) the dimensionless spin-glass correlation length ξ_{SG}/L , and (b) the dimensionless chiral-glass correlation length ξ_{CG}^+/L . The insets are magnified views of the low-temperature region.

Next, we examine the spin ordering. Fig.8(a) exhibits a finite-size scaling plot of the SG susceptibility, where the best value of ν_{SG} is estimated to be $\nu_{SG} = 0.9 \pm 0.2$. The value of ν_{SG} is consistent with the one determined above from the log-log plot of the SG susceptibility. In Fig.8(b), we show a scaling plot of the spin Binder ratio g_{SG} with $\nu_{SG} = 0.9$. The data collapse is rather poor here, however. The wavy structure of the g_{SG} curve observed for larger L turns out to deteriorate the data col-

lapse. The quality of the plot does not improve even with other choices of ν_{SG} . In Fig.8(c), we show a scaling plot of the dimensionless SG correlation length ξ_{SG}/L with $\nu_{SG} = 0.9$. Again, the data collapse is poor, and does not improve even with other choices of ν_{SG} .

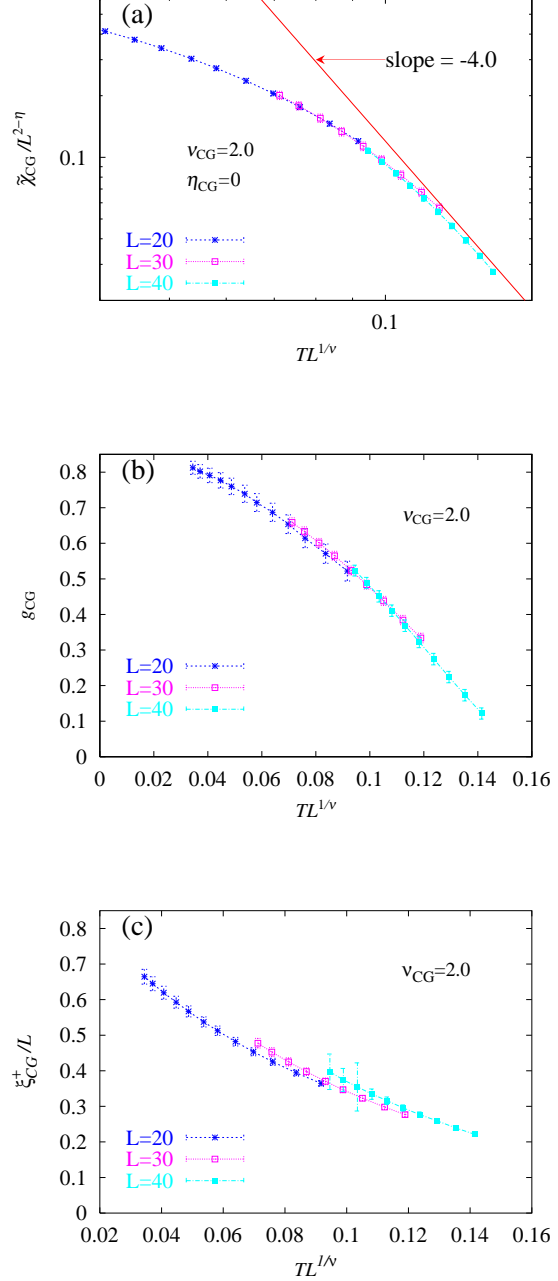


FIG. 7: Finite-size scaling plots of (a) the chiral-glass susceptibility, (b) the chiral Binder ratio, and (c) the dimensionless chiral-glass correlation length. The chiral-glass transition temperature is $T_{CG} = 0$.

Hence, although the SG susceptibility can be scaled by assuming $\nu_{SG} \simeq 0.9$, neither the spin Binder ratio nor

the SG correlation length can be scaled by the same ν_{SG} , nor by assuming any other ν_{SG} . Possible reason for this is either of the followings.

this case, $\nu_{\text{SG}} \simeq 0.9$ determined above from χ_{SG} is a true asymptotic exponent, and at low enough temperatures and for large enough sizes, both g_{SG} and ξ_{SG} should eventually scale with $\nu_{\text{SG}} \simeq 0.9$.

ii) The scaling behavior observed in χ_{SG} is somewhat accidental, not associated with the true asymptotic one. At low enough temperatures where ξ_{CG} well exceeds ξ_{SG} , the scaling behavior of χ_{SG} is changed into a different one characterized by a different ν_{SG} value, which would also scale both g_{SG} and ξ_{SG} at low enough temperatures and for large enough sizes. Unfortunately, the lack of our data in the low temperature regime $T \lesssim T_{\times}$ prevents us from giving any sensible estimate of the asymptotic ν_{SG} value. If the latter possibility ii) is really the case, there even exists a possibility that the spin-chirality decoupling eventually does not occur so that one has $\nu_{\text{SG}} = \nu_{\text{CG}}$. If one trusts our estimate of ν_{CG} given above, $\nu_{\text{CG}} \simeq 2.1$, the absence of the spin-chirality decoupling would then mean $\nu_{\text{SG}} \simeq 2.1$. Although we cannot completely rule out such a possibility, we also mention that any sign of such an equality $\nu_{\text{SG}} = \nu_{\text{CG}}$ was not seen in the available data.

At present, we cannot tell for sure which of the above possibilities, i) or ii), is really the case. Nevertheless, in view of the scaling observed in χ_{SG} , it seems to us that the above scenario ii) is rather unlikely, and the scenario i) is more plausible. Then, true asymptotic spin and chirality correlation-length exponents would not be far from $\nu_{\text{SG}} = 0.9 \pm 0.2$ and $\nu_{\text{CG}} = 2.1 \pm 0.3$ quoted above, which means the occurrence of the spin-chirality decoupling in the 2D Heisenberg SG. We note that these exponent values are close to the values reported in Ref.[7] for the same model by means of the $T = 0$ numerical domain-wall-energy calculation, $\nu_{\text{SG}} = 1.0 \pm 0.15$ and $\nu_{\text{CG}} = 2.1 \pm 0.2$.

SUMMARY

In summary, we performed large-scale equilibrium MC simulations of the 2D Heisenberg spin glass. Particular attention was paid to the behavior of the spin and the chirality correlation lengths. In order to observe the true asymptotic behavior, fairly large system size $L \gtrsim 20$ appears to be necessary. We have established that both the spin and the chirality order only at $T = 0$. The model seems to possess the two characteristic temperatures scales T^* and T_{\times} ($T^* > T_{\times} > 0$). Around T^* , the model enters into the chiral critical regime where critical fluctuations of the chirality become significant. This shows up as a changeover in the size dependence of the chiral correlation length or the CG susceptibility: Namely, above T^* , ξ_{CG} and $\tilde{\chi}_{\text{CG}}$ tend to decrease with L , whereas below T^* they tend to increase with L . The non-critical behavior observed above T^* might be understood as a mean-field-like behavior, as argued in Ref.[17]. The

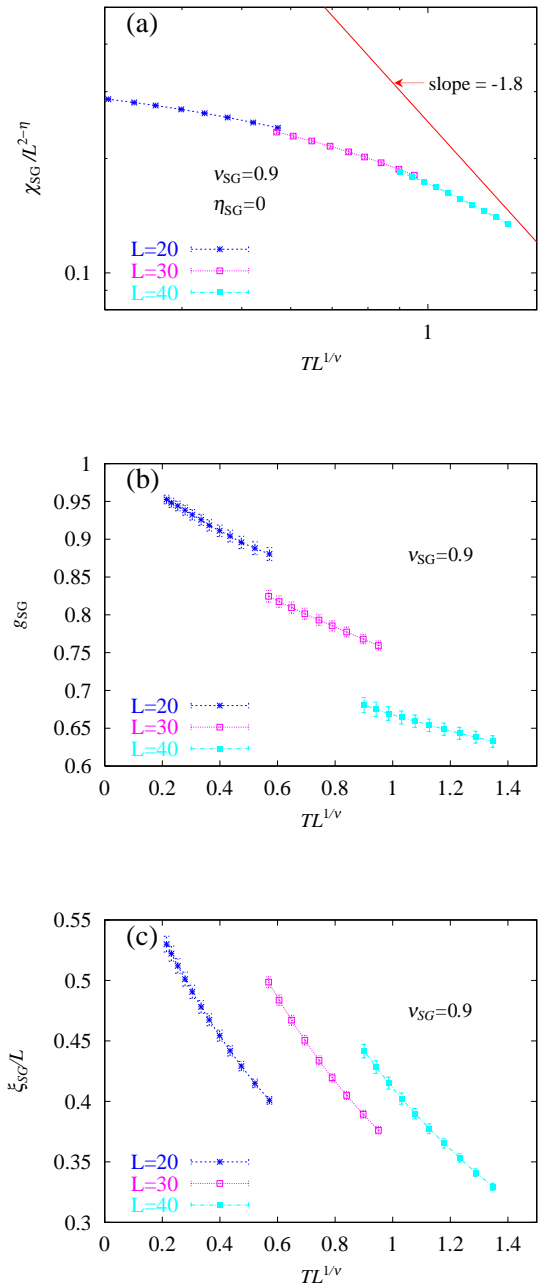


FIG. 8: Finite-size scaling plots of (a) the spin-glass susceptibility, (b) the spin Binder ratio, and (c) the dimensionless spin-glass correlation length. The transition temperature is $T_{\text{SG}} = 0$.

i) The width of the critical regime associated with the $T = 0$ SG transition depends on the physical quantities measured, being wide for the SG susceptibility but narrower for the Binder ratio or the correlation length. In

chiral correlation length, which stays shorter than the spin correlation length at high temperatures, catches up and exceeds the spin correlation length around the second characteristic temperature, $T_{\times} \simeq 0.01J$. Our data in the temperature regime $T_{\times} \lesssim T \lesssim T^*$ and for size $20 \lesssim L \lesssim 40$ yields the estimates of the spin and the chirality correlation-length exponents, $\nu_{\text{SG}} = 0.9 \pm 0.2$, $\nu_{\text{CG}} = 2.1 \pm 0.3$, respectively. Unfortunately, we don't have much data in the interesting temperature range $T \lesssim T_{\times}$, which prevents us from directly determining the truly asymptotic critical properties associated with the $T = 0$ transition. While we speculate that the asymptotic spin and the chirality exponents would not be far from the values quoted above, the data in the lower temperature regime $T \lesssim T_{\times} \simeq 0.01J$ and for larger sizes $L \gtrsim 40$ is required to settle the issue.

Acknowledgements

The numerical calculation was performed on the HITACHI SR8000 at the supercomputer system, ISSP, University of Tokyo. The authors are thankful to Dr. H. Yoshino and K. Hukushima for useful discussion.

-
- [1] For reviews on spin glasses, see *e. g.*, K. Binder and A. P. Young: *Rev. Mod. Phys.* **58** 801 (1986); K. H. Fischer and J. A. Hertz: *Spin Glasses* (Cambridge University Press, Cambridge, 1991); J. A. Mydosh: *Spin Glasses*, (Taylor & Francis, London-Washington DC, 1993); *Spin glasses and random fields*, ed. A. P. Young (World Scientific, Singapore, 1997).
- [2] J. A. Olive, A. P. Young and D. Sherrington, *Phys. Rev. B* **34**, 6341 (1986).

- [3] J. R. Banavar and M. Cieplak, *Phys. Rev. Lett.* **48**, 832 (1982).
- [4] W. L. McMillan, *Phys. Rev. B* **31**, 342 (1985).
- [5] F. Matsubara, T. Iyota and S. Inawashiro, *Phys. Rev. Lett.* **67**, 1458 (1991).
- [6] H. Yoshino and H. Takayama, *Europhys. Lett.* **22**, 631 (1993).
- [7] H. Kawamura, *Phys. Rev. Lett.* **68** 3785 (1992); *Int. J. Mod. Phys. C* **7**, 6341 (1996).
- [8] H. Kawamura, *J. Phys. Soc. Jpn.* **64**, 26 (1995).
- [9] H. Kawamura, *Phys. Rev. Lett.* **80**, 5421 (1998).
- [10] K. Hukushima and H. Kawamura, *Phys. Rev. E* **61**, R1008 (2000).
- [11] H. Kawamura and D. Imagawa, *Phys. Rev. Lett.* **87**, 207203 (2001).
- [12] D. Imagawa and H. Kawamura, *J. Phys. Soc. Jpn.* **71**, 127 (2002).
- [13] F. Matsubara, S. Endoh and T. Shirakura, *J. Phys. Soc. Jpn.* **69**, 1927 (2000); S. Endoh, F. Matsubara and T. Shirakura, *J. Phys. Soc. Jpn.* **70** 1543 (2001); F. Matsubara, T. Shirakura and S. Endoh, *Phys. Rev. B* **64**, 092412 (2001).
- [14] T. Nakamura and S. Endoh, *J. Phys. Soc. Jpn.* **71**, 2113 (2002).
- [15] L.W. Lee and A.P. Young, cond-mat/0302371.
- [16] K. Hukushima and H. Kawamura, unpublished.
- [17] D. Imagawa and H. Kawamura, *Phys. Rev. B* **67**, 224412 (2003) .
- [18] M. Schwartz and A.P. Young, *Europhys. Lett.* **15**, 209 (1991).
- [19] H. Kawamura and M. Tanemura, *J. Phys. Soc. Jpn.* **60**, 608 (1991).
- [20] P. Ray and M.A. Moore, *Phys. Rev. B* **45**, 5361 (1992).
- [21] H.S. Bokil and A.P. Young, *J. Phys. A* **29**, L89 (1996).
- [22] C. Wengel and A.P. Young, *Phys. Rev. B* **56**, 5918 (1997).
- [23] K. Hukushima and K. Nemoto, *J. Phys. Soc. Jpn.* **65**, 1604 (1995).